Acta Crystallographica Section B
Structural Science
ISSN 0108-7681

$Eu_3Si_{15-x}Al_{1+x}O_xN_{23-x}$ ($x \simeq 5/3$) as a commensurate composite crystal

Yuichi Michiue,[a]* Kousuke Shioi,[b] Naoto Hirosaki,[a] Takashi Takeda,[a] Rong-Jun Xie,[a] Akira Sato,[a] Mitsuko Onoda[a] and Yoshitaka Matsushita[c]

[a]National Institute for Materials Science, 1-1 Namiki, Tsukuba, Ibaraki 305-0044, Japan, [b]Corporate R&D Center, SHOWA DENKO K. K., 1-1-1 Ohnodai, Midori-ku, Chiba 267-0056, Japan, and [c]National Institute for Materials Science, Sayo-cho, Sayo, Hyogo 679-5148, Japan

Correspondence e-mail: michiue.yuichi@nims.go.jp

Received 28 May 2009
Accepted 31 July 2009

A new Eu-SiAlON crystal, $Eu_3Si_{15-x}Al_{1+x}O_xN_{23-x}$ ($x \simeq 5/3$), was found and the structure was determined by an X-ray diffraction technique using a twinned sample. The structure consists of a host framework, which is constructed by the connection of MX_4 tetrahedra (M: Si or Al; X: O or N), and Eu ions as the guest ions. The structure is considered to be a commensurate composite crystal. The basic vectors are $\mathbf{a}_1 = \mathbf{a}/3$, $\mathbf{b}$ and $\mathbf{c}$ for the first substructure, and $\mathbf{a}_2 = \mathbf{a}/5$, $\mathbf{b}$ and $\mathbf{c}$ for the second substructure. The first substructure consists of part of the host framework and the Eu ions, while the remainder of the host structure is taken as the second substructure. Possible phases belonging to the series are proposed using the composite crystal model in (3 + 1)-dimensional superspace. Chemical composition, possible space groups, cell parameters, and the basic model for those phases are presented.

1. Introduction

SiAlONs are well known as useful ceramics with mechanical hardness and thermal stability. In recent years much attention has been paid to rare-earth-doped SiAlON phosphors with promising luminescent properties (Xie *et al.*, 2002; van Krevel *et al.*, 2002; Xie, Hirosaki, Sakuma *et al.*, 2004; Xie, Hirosaki, Mitomo *et al.*, 2004; Hirosaki *et al.*, 2005). In addition to their importance as materials for practical use, SiAlONs are of interest from a crystal-chemistry viewpoint because of the variation in their structures. Some structures of SiAlON are closely related to those of nitrides; structures of α- and β-SiAlON, for example, derive from those of α- and β-Si_3N_4. New structure types which are not seen in nitrides are also reported, such as $SrSiAl_2O_3N_2$ (Lauterbach & Schnick, 1998), $Re_2Al_xSi_{12-x}N_{16-x}O_{2+x}$ (Re = Sr, Ba; $x \simeq 2$; Shen *et al.*, 1999; Esmaeilzadeh *et al.*, 2004), $Sr_{10}Sm_6Si_{30}Al_6O_7N_{54}$ (Lauterbach & Schnick, 2000) and $Sr_3Ln_{10}Si_{18}Al_{12}O_{18}N_{36}$ (Ln = Ce, Pr, Nd; Lauterbach *et al.*, 2000). In these structures MX_4 tetrahedra (M: Si or Al, X: O or N) are connected, forming a three-dimensional network or a host framework. Large cations, alkali-earth or rare-earth metal ions, are located at cavities of the host structure, and are considered to be the guest ions. Recently, a Sr-SiAlON, $Sr_5Al_{5+x}Si_{21-x}N_{35-x}O_{2+x}$ ($x \simeq 0$) with the space group $Pmn2_1$ was reported (Oeckler *et al.*, 2009). Although the structure has a typical feature of SiAlON consisting of the host framework of the MX_4 tetrahedra and the guest ions, two substructures with different periodicities along $\mathbf{a}$ of the ratio $a_1/a_2 = 8/5$ are seen.

In this study crystals of the new Eu-SiAlON, $Eu_3Si_{15-x}Al_{1+x}O_xN_{23-x}$ ($x \simeq 5/3$) with space group $P2_1$, were grown and the structure was determined using an X-ray diffraction technique. It was found that the structure consists of the two substructures which are basically identical to those

Table 1
Experimental details.

Experiments were carried out at 295 K with Mo $K\alpha$ radiation using a Bruker SMART APEX CCD area-detector diffractometer. Absorption was corrected for by multi-scan methods (*SADABS*; Sheldrick, 1996).

	3d	(3 + 1)-d
Crystal data		
Chemcial formula	$Al_{2.667}Eu_3N_{21.333}O_{1.667}Si_{13.333}$	$Al_{1.778}Eu_2N_{14.222}O_{1.111}Si_{8.889}$
M_r	1227.8	818.5
Crystal system, space group	Monoclinic, $P2_1$	Orthorhombic, $Pm2_1n(\alpha 00)$
a, b, c (Å)	14.6970 (9), 9.036 (2), 7.4677 (7)	4.8990 (3), 9.036 (2), 7.4677 (7)
β (°)	90.224 (1)	90
V (Å^3)	991.7 (2)	330.58 (8)
Z	2	1
μ (mm^{-1})	10.37	10.37
Crystal size (mm)	0.30 × 0.25 × 0.05	0.30 × 0.25 × 0.05
Data collection		
T_{min}, T_{max}	0.035, 0.432	0.035, 0.432
No. of measured, independent and observed [$I > 2\sigma(I)$] reflections	22 393, 10 994, 10 354	22 393, 10 994, 10 354
R_{int}	0.033	0.033
Refinement		
$R[F^2 > 2\sigma(F^2)]$, $wR(F^2)$, S	0.053, 0.115, 2.15	0.055, 0.119, 2.23
No. of parameters	266	248
No. of restraints	0	0
$\Delta\rho_{max}$ $\Delta\rho_{min}$ (e Å^{-3})	5.13, −3.47	4.59, −4.18

Computer programs used: *JANA*2006 (Petricek *et al.*, 2006).

seen in the above-mentioned $Sr_5Al_{5+x}Si_{21-x}N_{35-x}O_{2+x}$ ($x \simeq 0$), although the a_1/a_2 ratio in $Eu_3Si_{15-x}Al_{1+x}O_xN_{23-x}$ ($x \simeq 5/3$) is 5/3. From the viewpoint of higher-dimensional crystallography, the two SiAlON structures (ignoring the difference in guest ions Eu and Sr) are considered as commensurate phases belonging to a series of composite crystals. Therefore, two methods were used for the description of the $Eu_3Si_{15-x}Al_{1+x}O_xN_{23-x}$ ($x \simeq 5/3$) structure; one was the conventional method in three-dimensional space, and another was the (3 + 1)-dimensional description based on the superspace formalism (van Smaalen, 1995; Yamamoto, 1996). The (3 + 1)-dimensional structure model proposed in this study is suitable for the unified description of structures in the series and makes it easier for us to predict the chemical composition, space group, cell parameters and the basic structure model for other possible phases.

2. Experimental

A powder sample with the nominal composition $Eu_6Si_{27}Al_6O_6N_{42}$ was prepared from α-Si_3N_4 (SN-E10, Ube Industries Ltd), AlN (type F, Tokuyama Co., Ltd) and Eu_2O_3 (Shin-Etsu Chemical Co., Ltd). The mixed powder was placed into an hBN crucible and then sintered in a graphite resistance furnace at 2173 K for 24 h under 1 MPa nitrogen atmosphere. Pale-yellow crystals of Eu-SiAlON were obtained along with polycrystalline products. The chemical composition $Eu_{6.4}Si_{33.2}Al_{6.7}O_{3.2}N_{50.5}$ was given for the crystals by EPMA (electron probe microanalysis) measurements.

Diffraction intensities were collected on a CCD area detector (Bruker SMART APEX). Conditions and parameters for data collection and refinement are listed in Table 1. Although the Laue class *mmm* was suggested by diffraction intensities, it was concluded during the refinements that the sample was a twin of the monoclinic structure with $\beta \simeq 90°$ in the space group $P2_1$. Considering anomalous dispersion for the noncentrosymmetric structure, four domains were taken into account for the refinements. Volume fractions were 0.258, 0.251 (10), 0.246 (10) and 0.245 (10) with the twin operations $(-x, y, z)$ for the second fragment, $(-x, -y, -z)$ for the third, and $(x, -y, -z)$ for the fourth.

The structure was first treated as a conventional three-dimensional structure. Positions of metal ions were determined by the charge-flipping method using *SUPERFLIP* (Palatinus & Chapuis, 2007) incorporated in *JANA*2006 (Petricek *et al.*, 2006). The remaining ions were located using Fourier and difference-Fourier syntheses. Determination of occupation factors of Si and Al at the framework metal site is difficult for the present structure containing many nonequivalent positions. Therefore, the Si/Al ratio at the sites was uniformly fixed to 5.0, which was estimated by the EPMA measurements of the crystals. It is suggested from the EPMA result that occupation factors at Eu sites are less than the unity. However, full occupation was assumed at all Eu sites because the refinement with the vacancy at these sites gave no improvement in reliability factors. Considering the charge neutrality of a whole crystal, the N/O ratio was estimated at 12.8, that is $x \simeq 5/3$ in the chemical formula $Eu_3Si_{15-x}Al_{1+x}O_xN_{23-x}$. Programs used were *JANA*2006 (Petricek *et al.*, 2006) for calculations, and *VESTA* (Momma & Izumi, 2008) and *ATOMS* (Dowty, 2005) for graphics.

In order to confirm that the crystal system of the structure is not orthorhombic but monoclinic, X-ray powder diffraction measurements were taken using a synchrotron radiation facility. As the products were always a mixture of crystals of $Eu_3Si_{15-x}Al_{1+x}O_xN_{23-x}$ ($x \simeq 5/3$) and polycrystalline samples of other phases, crystals of $Eu_3Si_{15-x}Al_{1+x}O_xN_{23-x}$ ($x \simeq 5/3$) were separated by picking them up by hand. Several tens of the single crystals were collected and ground down. The specimen was sealed into a quartz capillary tube with an inner diameter of 0.3 mm. X-ray diffraction data were collected using a high-resolution diffractometer (Tanaka *et al.*, 2008) with Debye–Scherer geometry installed at the BL15XU beamline at SPring-8. The measurement was carried out with a wavelength of 0.65297 Å over a 2θ range up to 60°. Structure

parameters were fixed to the values determined by the single-crystal diffraction technique, and other parameters such as cell parameters, background and peak profile parameters were refined by the profile fitting using *JANA*2006 (Petricek *et al.*, 2006). Deviation of β from 90° was clear in some parts of the diffraction diagram, and the β value obtained was 90.224 (1)°. Final reliability factors were R_p = 0.0141 and R_{wp} = 0.0286. Refinement by keeping β = 90° deteriorated the fitting; R_p = 0.0168 and R_{wp} = 0.0348.

3. Description of the structure

In this section the structure of $Eu_3Si_{15-x}Al_{1+x}O_xN_{23-x}$ ($x \simeq 5/3$) is treated as a conventional three-dimensional structure. Final structural parameters are given as supplementary materials.[1] For convenience, metal ions constructing the framework structure, that is Si and Al, are represented by *M*, and anions, N and O, are by *X*, hereafter. It was found that the *M*3 site splits into two positions, *M*3a and *M*3b. Only one of the two sites is occupied in local structures, as the distance between the two sites is less than 1 Å. Another site, *M*6, also splits into two positions, *M*6a and *M*6b. It was assumed that *X* sites interconnecting three MX_4 tetrahedra were fully occupied by N as seen for the standard SiAlON structures. These anion sites are expressed as N4–N23 (Table S1 in supplementary materials), while the remaining sites, *X*1–*X*3, are partially occupied by O and N.

The structure of $Eu_3Si_{15-x}Al_{1+x}O_xN_{23-x}$ ($x \simeq 5/3$) projected along **a** is given in Fig. 1. A host framework consists of *M* (*i.e.* Si or Al) and *X* (*i.e.* O or N) ions, while Eu ions are located in cavities as guest ions. The host structure is constructed by the connection of MX_4 tetrahedra. To understand the unique character of the structure, it is helpful to divide the host structure into two parts as indicated in Fig. 1. The first unit projected along **c** is given in Fig. 2(*a*) along with the Eu ions. In this figure *M*3a and *M*6a sites are occupied and consequently *M*3b and *M*6b sites are vacant as an example of the possible local structure. MX_4 tetrahedra are connected sharing the vertex or edge, forming rings consisting of six MX_4 tetrahedra. It should be noted that the arrangement of Eu and *M* ions approximates to that at regular intervals of *a*/3 = 4.899 Å, as illustrated in the figure. That is, the structure of metal ions in Fig. 2(*a*) is taken as a threefold superstructure along **a**. A sublattice is defined by taking the *a* axis $\mathbf{a}_1 = \mathbf{a}/3$, and *b* and *c* axes are common to those of the superlattice. Anion sites, *X*1, *X*2 and *X*3, are also included in the same substructure, because these have a similar periodicity to that of the metal sites, as indicated in Fig. 2(*a*). On the other hand, the remaining anion sites in Fig. 2(*a*) are allotted for another substructure which will be mentioned below. The projection of the second part along **c** is given in Fig. 2(*b*), which is the simple connection of MN_4 tetrahedra sharing vertices. It is obvious that the structure is considered as a fivefold superstructure, because the repetition of five MN_4 tetrahedra along **a** is seen. Thus, a sublattice for this substructure is defined by taking the *a* axis $\mathbf{a}_2 = \mathbf{a}/5$. In higher-dimensional crystallography, the structure mentioned above is well known as a composite crystal, in which (at least) two substructures with different periodicities coexist (van Smaalen, 1995; Yamamoto, 1996). In the present case the whole structure consists of two substructures, and their periodicities are different along **a**. The structure description as a composite crystal will be given in the following section.

Eu—*X* distances less than 3.3 Å and *M*—*X* distances in each MX_4 tetrahedron are listed in Table 2. One of the *M*—N distances is longer than 2 Å for *M*3a and *M*3b, which is unusual for SiAlONs. Bond-valence sums (BVSs) for Eu and *M* sites are given in Table 3. Parameters for the BVS calculation were taken from the literature (Brown, 1996). Despite

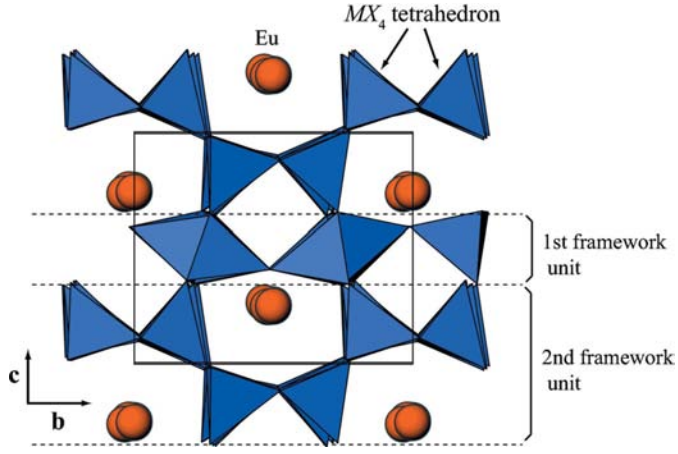

Figure 1
Structure of $Eu_3Si_{15-x}Al_{1+x}O_xN_{23-x}$ ($x \simeq 5/3$) projected along **a**. Structure parameters used are in the supplementary material. *M*3a and *M*6a are occupied, but *M*3b and *M*6b are vacant as an example of the possible local structure.

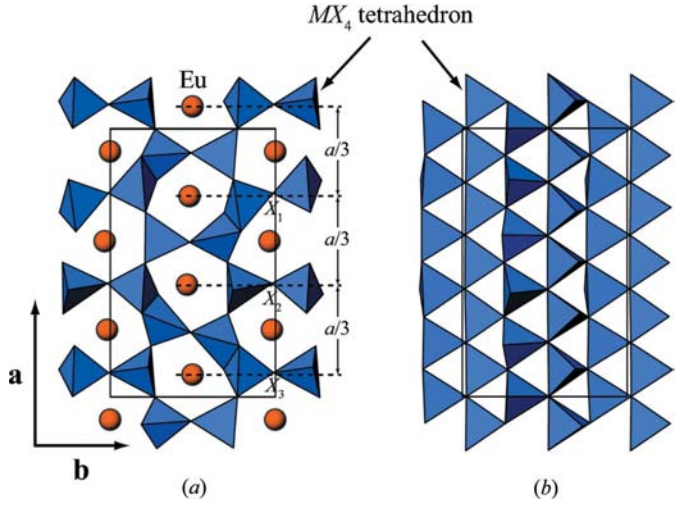

Figure 2
Projections along **c** of (*a*) the first framework unit and Eu ions, and (*b*) the second framework unit in $Eu_3Si_{15-x}Al_{1+x}O_xN_{23-x}$ ($x \simeq 5/3$).

[1] Supplementary data for this paper are available from the IUCr electronic archives (Reference: SN5084). Services for accessing these data are described at the back of the journal.

Table 2
Selected interatomic distances (Å) in $Eu_3Si_{15-x}Al_{1+x}O_xN_{23-x}$ ($x \simeq 5/3$).

Eu1—$X1^{i}$	2.811 (6)	Eu2—$X2^{ii}$	2.568 (6)	Eu3—$X1^{ii}$	2.657 (6)
Eu1—$X3^{ii}$	2.584 (6)	Eu2—$X3^{ii}$	2.839 (6)	Eu3—$X2^{ii}$	2.806 (6)
Eu1—N4	2.563 (6)	Eu2—N5	3.020 (5)	Eu3—N7	2.683 (7)
Eu1—$N9^{iii}$	2.821 (6)	Eu2—N6	2.664 (7)	Eu3—$N10^{iv}$	2.657 (6)
Eu1—$N13^{iv}$	3.098 (9)	Eu2—N11	3.268 (6)	Eu3—$N15^{iv}$	3.025 (6)
Eu1—$N14^{v}$	2.874 (5)	Eu2—$N12^{iv}$	2.568 (6)	Eu3—N17	2.887 (6)
Eu1—$N18^{iv}$	2.937 (5)	Eu2—$N16^{v}$	3.137 (6)	Eu3—$N20^{vii}$	2.785 (5)
Eu1—$N19^{vi}$	3.023 (6)	Eu2—$N22^{vii}$	2.741 (5)		
$M1$—$X1^{viii}$	1.686 (5)	$M2$—$X2^{viii}$	1.702 (6)	$M3$a—$X3^{viii}$	1.691 (8)
$M1$—N4	1.709 (6)	$M2$—N5	1.769 (6)	$M3$a—N7	1.755 (9)
$M1$—N9	1.756 (6)	$M2$—N6	1.783 (8)	$M3$a—N8	2.033 (9)
$M1$—N10	1.803 (6)	$M2$—N11	1.740 (6)	$M3$a—N13	1.723 (10)
$M3$b—$X3^{viii}$	1.756 (9)	$M4$—$X2^{ii}$	1.715 (7)	$M5$—$X1^{ii}$	1.692 (5)
$M3$b—N7	1.689 (10)	$M4$—N6	1.735 (8)	$M5$—N8	1.675 (8)
$M3$b—N12	2.023 (9)	$M4$—N7	1.756 (8)	$M5$—$N9^{ix}$	1.736 (6)
$M3$b—N13	1.774 (10)	$M4$—N12	1.698 (6)	$M5$—N13	1.800 (10)
$M6$a—$X3^{ii}$	1.761 (8)	$M6$b—$X3^{ii}$	1.711 (9)	$M7$—$N8^{iv}$	1.675 (8)
$M6$a—N5	1.725 (7)	$M6$b—N4	1.897 (7)	$M7$—$N18^{x}$	1.770 (5)
$M6$a—N10	1.806 (7)	$M6$b—N5	1.768 (7)	$M7$—$N19^{iii}$	1.777 (6)
$M6$a—N11	1.840 (7)	$M6$b—N10	1.735 (8)	$M7$—$N23^{iv}$	1.786 (6)
$M8$—$N7^{iv}$	1.786 (8)	$M9$—$N6^{iv}$	1.774 (7)	$M10$—$N5^{iv}$	1.725 (6)
$M8$—$N17^{x}$	1.737 (6)	$M9$—$N16^{x}$	1.716 (6)	$M10$—$N15^{x}$	1.767 (6)
$M8$—$N22^{iv}$	1.763 (6)	$M9$—$N21^{iv}$	1.73 (7)	$M10$—$N20^{iv}$	1.747 (6)
$M8$—$N23^{iv}$	1.739 (6)	$M9$—$N22^{iv}$	1.789 (6)	$M10$—$N21^{iv}$	1.770 (7)
$M11$—$N4^{iv}$	1.751 (6)	$M12$—$N9^{iii}$	1.760 (6)	$M13$—$N13^{iv}$	1.731 (10)
$M11$—$N14^{x}$	1.755 (5)	$M12$—$N14^{iii}$	1.753 (7)	$M13$—$N17^{iv}$	1.746 (7)
$M11$—$N19^{iv}$	1.778 (6)	$M12$—$N18^{iv}$	1.803 (6)	$M13$—$N18^{iv}$	1.751 (6)
$M11$—$N20^{iv}$	1.783 (6)	$M12$—$N19^{xi}$	1.729 (6)	$M13$—$N20^{xi}$	1.766 (5)
$M14$—$N12^{iv}$	1.716 (6)	$M15$—$N11^{iv}$	1.699 (6)	$M16$—$N10^{iv}$	1.771 (6)
$M14$—$N16^{iv}$	1.799 (7)	$M15$—$N15^{iv}$	1.801 (7)	$M16$—$N14^{iv}$	1.746 (7)
$M14$—$N17^{iv}$	1.804 (7)	$M15$—$N16^{iv}$	1.789 (7)	$M16$—$N15^{iv}$	1.762 (7)
$M14$—$N21^{xi}$	1.756 (5)	$M15$—$N22^{xi}$	1.775 (5)	$M16$—$N23^{xi}$	1.735 (5)

Symmetry codes: (i) $-x, y-\frac{1}{2}, -z+1$; (ii) $-x+1, y-\frac{1}{2}, -z+1$; (iii) $-x, y+\frac{1}{2}, -z+1$; (iv) $-x+1, y+\frac{1}{2}, -z+1$; (v) $x, y, z-1$; (vi) $-x, y+\frac{1}{2}, -z$; (vii) $-x+1, y+\frac{1}{2}, -z$; (viii) $x, y-1, z$; (ix) $x+1, y, z$; (x) $-x+1, y+\frac{1}{2}, -z+2$; (xi) $x, y+1, z$.

Table 3
Bond-valence sum for metal sites in $Eu_3Si_{15-x}Al_{1+x}O_xN_{23-x}$ ($x \simeq 5/3$).

	BVS
Eu1	2.147 (12)
Eu2	2.259 (14)
Eu3	2.043 (13)

	M = Si	M = Al
$M1$	3.77 (3)	4.42 (3)
$M2$	3.62 (3)	4.23 (4)
$M3$a	3.31 (4)	3.85 (5)
$M3$b	3.22 (4)	3.76 (5)
$M4$	3.85 (4)	4.51 (4)
$M5$	3.87 (4)	4.53 (4)
$M6$a	3.31 (3)	3.89 (4)
$M6$b	3.38 (3)	3.96 (4)
$M7$	3.74 (3)	4.47 (4)
$M8$	3.67 (3)	4.39 (4)
$M9$	3.72 (3)	4.45 (4)
$M10$	3.71 (3)	4.43 (4)
$M11$	3.57 (3)	4.26 (3)
$M12$	3.63 (3)	4.33 (4)
$M13$	3.75 (4)	4.48 (5)
$M14$	3.56 (3)	4.26 (4)
$M15$	3.59 (3)	4.29 (4)
$M16$	3.69 (3)	4.42 (4)

the different numbers of coordinated anions, the BVSs for all the three Eu sites are roughly close to the formal charge of Eu^{2+}. BVSs at the M sites were calculated for the two cases. In the first case, the M sites were occupied by Si ions, while occupation by Al ions was assumed in the second case. BVSs in the first case are moderately lower that 4, the formal charge of Si^{4+}. The BVSs at $M3$a, $M3$b, $M6$a and $M6$b sites are lower than those at the other sites. This suggests that the Si/Al ratios at these metal sites are lower than those at the other M sites. BVSs in the second case far exceed the formal charge of Al^{3+} at all the M sites, implying that all the MX_4 tetrahedra are basically too small for the Al ion to be stabilized.

The structure of $Eu_3Si_{15-x}Al_{1+x}O_xN_{23-x}$ ($x \simeq 5/3$) is closely related to that of an Eu-doped $Sr_5Al_{5+x}Si_{21-x}N_{35-x}O_{2+x}$ ($x \simeq 0$), with an orthorhombic unit cell of a = 23.614, b = 7.487 and c = 9.059 Å, and the space group $Pmn2_1$ (Oeckler *et al.*, 2009). The two framework units which are basically identical to those in Figs. 2(*a*) and (*b*) are seen, but the ratio of basic periods for the two substructures is a_1/a_2 = 8/5 in $Sr_5Al_{5+x}Si_{21-x}N_{35-x}O_{2+x}$ ($x \simeq 0$). It is obvious that the structure of $Sr_5Al_{5+x}Si_{21-x}N_{35-x}O_{2+x}$ ($x \simeq 0$) can also be treated as a commensurate composite crystal, although the refinement by Oeckler *et al.* (2009) was based on a conventional method in three-dimensional space. Despite different crystal systems and space groups, the two structures $Eu_3Si_{15-x}Al_{1+x}O_xN_{23-x}$ ($x \simeq 5/3$) and $Sr_5Al_{5+x}Si_{21-x}N_{35-x}O_{2+x}$ ($x \simeq 0$) are derived from the identical structure model in (3 + 1)-dimensional space as shown in following sections.

4. (3 + 1)-dimensional superspace description as a composite crystal

It has been proved from many studies (van Smaalen, 1987; Yamamoto *et al.*, 1985; Perez-Mato *et al.*, 1987) that the superspace formalism, which was originally developed for the analysis of incommensurate structures (de Wolff, 1974; Janner & Janssen, 1980*a*,*b*), is useful for the description of commensurate structures. In this section, in order to clarify the character of $Eu_3Si_{15-x}Al_{1+x}O_xN_{23-x}$ ($x \simeq 5/3$) as a commensurate composite crystal, the structure was treated as a compositely modulated structure and refined based on the well established (3 + 1)-dimensional superspace method. Two basic cells with common **b** and **c** were used. The first substructure is defined by basic vectors $\mathbf{a}_1 = \mathbf{a}/3$, **b** and **c**, while those for the second substructure are $\mathbf{a}_2 = \mathbf{a}/5$, **b** and **c**. There are several different possibilities when taking a (3 + 1)-dimensional superspace group which is consistent with the space group $P2_1$ for a commensurate phase in three-dimensional space. Considering the space group $Pm2_1n$ for $Sr_5Al_{5+x}Si_{21-x}N_{35-x}O_{2+x}$ ($x \simeq 0$) ($Pmn2_1$ in the setting by Oeckler *et al.*, 2009), the superspace group $Pm2_1n(\alpha 00)$ is suitable for the unified description of the structures, because the space group of a commensurate structure at the three-

Table 4
Space groups derived from the superspace group $Pm2_1n(\alpha00)$.

	$t_0 = 0$ (modulo 1/2m)	$t_0 = 1/4m$ (modulo 1/2m)	t_0 = general
$\alpha = n/m$ = odd/odd	$P12_11$	$Pm11$	$P1$
odd/even	$P12_11$	$Pm11$	$P1$
even/odd	$Pm2_1n$	$Pm2_1n$	$P11n$

The origin is shifted by (1/4, 0, 0, 0) from that in the standard setting of $Pm2_1n(\alpha00)$.

dimensional section $t_0 = 0$ of $Pm2_1n(\alpha00)$ is $P2_1$ for α ($= a_2^*/a_1^* = a_1/a_2$) = 5/3 (α = odd/odd in general), and $Pm2_1n$ for α = 8/5 (α = even/odd). Variation of space groups at three-dimensional sections are summarized in Table 4. In a three-dimensional structure derived from the (3 + 1)-dimensional model of the superspace group $Pm2_1n(\alpha00)$, β is fixed at 90° even for the monoclinic phase. Strictly speaking, β deviates slightly from 90° in the real structure of $Eu_3Si_{15-x}Al_{1+x}O_xN_{23-x}$ ($x \simeq 5/3$), as mentioned in §2. In this sense, the structure model using the superspace group $Pm2_1n(\alpha00)$ is not real but an approximation. A more accurate structure would be given by taking a monoclinic model of the superspace group $P2_1(\alpha0\gamma)$, but we chose the model of $Pm2_1n(\alpha00)$ for the following reasons. First, the superspace group $Pm2_1n(\alpha00)$ is suitable for a unified description of the structures in the series. Second, the deviation of β from 90° is so small that the structure obtained from $Pm2_1n(\alpha00)$ is identical to that from $P2_1(\alpha0\gamma)$ in practice. Third, the description by an orthorhombic model in (3 + 1)-dimensional superspace gives an explanation for the fact that β is close to 90° in the monoclinic structure. Also, twinning is likely to occur in crystal growth of monoclinic structures which derive

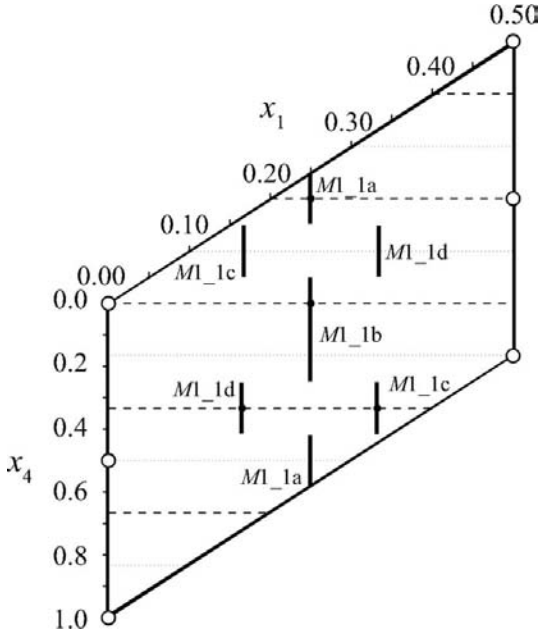

Figure 3
Occupation domains of *M*1_1a–*M*1_1d sites for the basic structure projected on the x_1–x_4 plane. Parameters used are in Table 5.

Table 5
Parameters for the basic structure of $Eu_3Si_{15-x}Al_{1+x}O_xN_{23-x}$ ($x \simeq 5/3$) in (3 + 1)-dimensional superspace.

Values with asterisks are isotropic ADPs (U_{iso}), while the values without asterisks are the equivalent ADPs (U_{eq}).

Atom	x_1^0	x_2^0	x_3^0	x_4^0	Δ	U_{iso}^*/U_{eq} (Å^2)
First substructure						
Eu1_1	0.25	0.5	0.25486 (3)			0.03111 (7)
*M*1_1a	0.25	0.1662 (3)	0.4901 (3)	0	1/3	0.0113 (5)
*M*1_1b	0.25	0.1911 (3)	0.5558 (3)	0.5	1/3	0.0138 (5)
*M*1_1c	0.1678 (8)	0.1674 (4)	0.4895 (5)	0.1131 (13)	1/6	0.0009 (7)*
*M*1_1d	0.3348 (11)	0.1845 (5)	0.5596 (7)	0.3913 (18)	1/6	0.0053 (10)*
*M*1_2a	0.75	0.3404 (2)	0.5149 (3)	0.5	1/3	0.0110 (4)
*M*1_2b	0.75	0.3126 (2)	0.4419 (3)	0	1/3	0.0115 (5)
*M*1_2c	0.8293 (9)	0.3387 (5)	0.5134 (6)	0.3822 (15)	1/6	0.0105 (9)*
*M*1_2d	0.6644 (10)	0.3182 (5)	0.4443 (6)	0.1073 (16)	1/6	0.0070 (9)*
*X*1_1	0.25	0.0019 (5)	0.5905 (3)			0.0189 (5)*
Second substructure						
*M*2_1	0.5	0.64182 (10)	0.85767 (9)			0.00978 (16)
*M*2_2	0	0.84351 (10)	0.13046 (9)			0.00973 (16)
N2_1	0.5	0.2237 (3)	0.3520 (3)			0.0152 (5)*
N2_2	0	0.2837 (3)	0.6502 (3)			0.0122 (4)*
N2_3	0.5	0.2781 (2)	0.9769 (3)			0.0144 (3)*
N2_4	0	0.0365 (2)	0.1125 (3)			0.0128 (3)*

Occupation factors are Si/Al = 0.8333/0.1667 for *M*1_1a, *M*1_1b, *M*1_2a and *M*1_2b, and 0.441 (6)/0.0882 for *M*1_1c, 0.392 (6)/0.0785 for *M*1_1d, 0.442 (6)/0.0884 for *M*1_2c, and 0.391 (6)/0.0783 for *M*1_2d. x_4^0 is generally given by $1/4 + \alpha(x_1^0 - 1/4)$ for *M*1_1c and *M*1_1d, and by $1/4 + \alpha(x_1^0 - 3/4)$ for *M*1_2c and *M*1_2d.

from an orthorhombic model in (3 + 1)-dimensional space. A similar situation was reported for the threefold superstructure of Cs_2HgCl_4 (Bagautdinov *et al.*, 1999); a twinning monoclinic structure of $P2_1/a$ was refined using an orthorhombic (3 + 1)-dimensional model of the superspace group $Pnma(00\gamma)0s0$.

The origin is taken on a screw axis, and symmetry operations are x_1, x_2, x_3, x_4; $\frac{1}{2}+x_1, \frac{1}{2}+x_2, -x_3, x_4$; $\frac{1}{2}-x_1, x_2, x_3, -x_4$; $-x_1, \frac{1}{2}+x_2, -x_3, -x_4$. [Note that the origin is shifted by (1/4, 0, 0, 0) from that in the standard setting of $Pm2_1n(\alpha00)$.] $Pm2_1n(\alpha00)$ is equivalent to $P2_1nm(00\gamma)$ (No. 31.5) in *International Tables for Crystallography*, Vol. C (Janssen *et al.*, 1999). Parameters for the basic structure of the (3 + 1)-dimensional description are given in Table 5. Fourier coefficients for displacive modulations and anisotropic displacement parameters are given as supplementary materials. The first substructure basically consists of one Eu, two *M* and one *X* sites, and the second substructure contains two *M* and four N sites. Considering the splitting of part of the framework metal sites, the box-shaped function, *i.e.* the so-called crenel function, was used for the occupational modulation functions of the *M* sites in the first substructure. The refined structure is practically identical to that from the three-dimensional refinement, and reliability factors are $R_{obs}(F) = 0.058$, $wR_{obs}(F^2) = 0.118$, $R_{all}(F) = 0.059$ and $wR_{all}(F^2) = 0.119$ for 248 parameters. The number of refined parameters in the (3 + 1)-dimensional refinement is less than that in the three-dimensional refinement (266) because modulations for isotropic ADPs are not considered in (3 + 1)-dimensional refinements using *JANA*2006. For example, isotropic ADPs for the three *X* sites (*X*1, *X*2 and *X*3 in a three-dimensional description) were set to the same value in the (3 + 1)-dimensional refinement,

while these parameters were independently refined in three-dimensional analysis.

As the crenel function is used for M sites in the first substructure, parameters for occupation domains (or atomic surfaces) should be determined so that neighbouring occupation domains connect without duplication or voids along t (= $x_4 - \alpha x_1$). For example, four M sites, $M1$, $M2$, $M3$a and $M3$b in three-dimensional refinement, are allotted for the $M1\_1$ site in the (3 + 1)-dimensional model, which is actually divided into four sites, $M1_1$a-$M1_1$d, using the crenel function in Table 5. These occupation domains are projected on the x_1–x_4 plane (Fig. 3), which fulfils the above condition. $M1_1$a and $M1_1$b correspond to $M2$ and $M1$ in the three-dimensional model. Only one of the M1_1c and M1_1d sites, corresponding to $M3$a and $M3$b in the three-dimensional model, is occupied in real local structures. The description of the splitting of the M site in the (3 + 1)-dimensional model will be discussed again in the following section.

As is usually seen in composite crystals, the two substructures interact with each other giving rise to the displacive modulation. Modulation functions of the fractional coordinate x for all atoms in the second substructure are given in Fig. 4. Displacements for N2_1 and N2_2 are prominent, which is reasonably explained by the fact that these anions coordinate to M ions of not only the second substructure, but also the first substructure. In other words these anions connect the two framework units in Fig. 1, being located at the border (dotted lines in the figure). On the other hand, modulations for the other anions in the second substructure are small, implying a weak interaction for these atoms with the first substructure. This is simply because these anions coordinate to M ions of only the second substructure.

5. Discussion

It is obvious that $Eu_3Si_{15-x}Al_{1+x}O_xN_{23-x}$ ($x \simeq 5/3$) and $Sr_5Al_{5+x}Si_{21-x}N_{35-x}O_{2+x}$ ($x \simeq 0$) are considered as members of a series of composite crystals, ignoring the difference in species of guest ions, Eu and Sr. The basic structure for $Sr_5Al_{5+x}Si_{21-x}N_{35-x}O_{2+x}$ ($x \simeq 0$) with space group $Pm2_1n$ can be drawn using the (3 + 1)-dimensional model in Table 5 with a few modifications. First, the wave-vector component α (= a_1/a_2) should be changed to 8/5. Next, parameters for splitting M sites should be considered. The M site splitting is also seen in $Sr_5Al_{5+x}Si_{21-x}N_{35-x}O_{2+x}$ ($x \simeq 0$; Oeckler *et al.*, 2009). As mentioned in §4, parameters for occupation domains should be defined so that neighbouring occupation domains connect without duplication or voids along t (= $x_4 - \alpha x_1$). According to structure data reported by Oeckler *et al.* (2009), among five M sites allotted for $M1\_1$ in the (3 + 1)-dimensional model, two M sites are split. Therefore, the width of the occupation domain Δ should be 3/10, 3/10, 1/5 and 1/5 for $M1_1$a, $M1_1$b, $M1_1$c and $M1_1$d. Centers of the occupation domain (x_4^0) for these sites are given by general equations in the footnote of Table 5. Occupation domains of $M1_1$a–$M1_1$d sites, which were modified for $Sr_5Al_{5+x}Si_{21-x}N_{35-x}O_{2+x}$ ($x \simeq 0$), are shown in Fig. 5. The same modification should also be made for $M1_2$a–$M1_2$d sites. The structure model is basically identical to that given by Oeckler *et al.* (as Fig. 4*a* in their paper) and is obtained at the three-dimensional section $t_0 = 0$ of the modified (3 + 1)-dimensional model assuming that $M1_1$c and $M1_2$d are occupied and consequently $M1_1$d and $M1_2$c are vacant.

The basic periods of the second substructure along **a** for the two compounds are close to each other; a_2 = 14.697/5 = 2.939 Å for $Eu_3Si_{15-x}Al_{1+x}O_xN_{23-x}$ ($x \simeq 5/3$) and a_2 = 23.614/8 = 2.952 Å for $Sr_5Al_{5+x}Si_{21-x}N_{35-x}O_{2+x}$ ($x \simeq 0$). On the other hand, the difference in the basic period of the first substructure is rather large between $Eu_3Si_{15-x}Al_{1+x}O_xN_{23-x}$

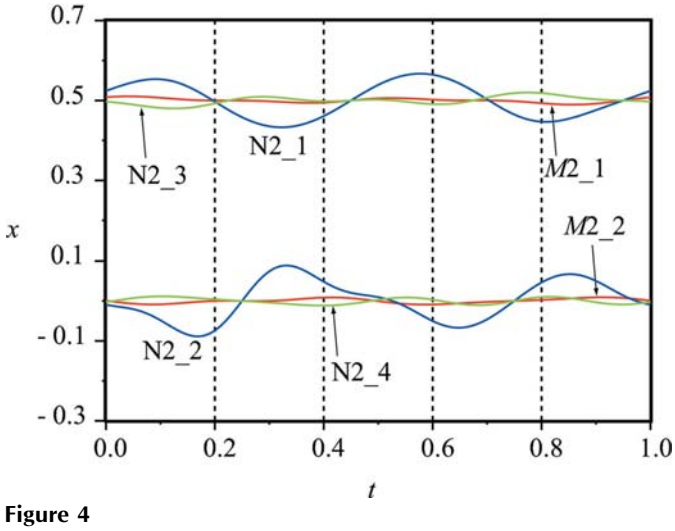

Figure 4
Modulations of the fractional coordinate x for atoms in the second substructure of $Eu_3Si_{15-x}Al_{1+x}O_xN_{23-x}$ ($x \simeq 5/3$).

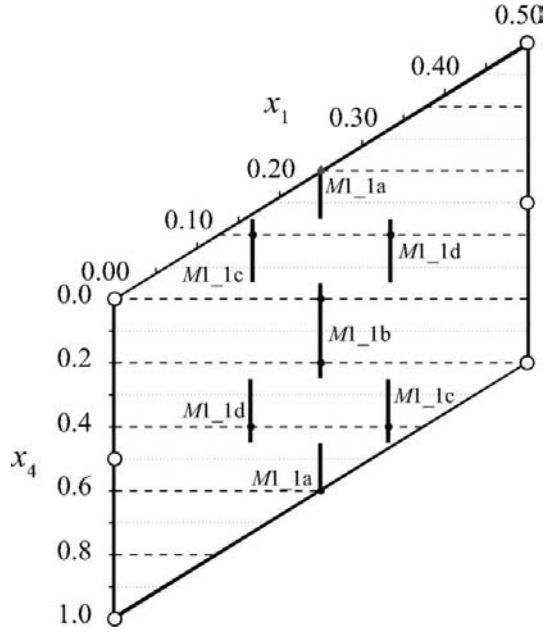

Figure 5
Occupation domains of $M1_1$a–$M1_1$d sites modified for $Sr_5Al_{5+x}Si_{21-x}N_{35-x}O_{2+x}$ ($x \simeq 0$) of α = 8/5. Displacive modulations are ignored.

($x \simeq 5/3$) and $Sr_5Al_{5+x}Si_{21-x}N_{35-x}O_{2+x}$ ($x \simeq 0$); a_1 = 14.697/3 = 4.899 Å for the former and a_1 = 23.614/5 = 4.722 Å for the latter. This means that the first substructure is more flexible than the second substructure. Structures for any members of the composite crystal series with the desired a_1/a_2 ratios are drawn by the (3 + 1)-dimensional model based on Table 5. However, it is unclear which of the derived structures are actually formed. As seen above, the second substructure is rigid and its basic period along **a** seems to be fixed at around a_2 = 2.94–2.95 Å. Although the first substructure has flexibility to a certain extent, it seems that the a_1/a_2 ratio in real structures is limited over a certain range. At least two structures of a_1/a_2 = 5/3 and a_1/a_2 = 8/5, that is $Eu_3Si_{15-x}Al_{1+x}O_xN_{23-x}$ ($x \simeq 5/3$) and $Sr_5Al_{5+x}Si_{21-x}N_{35-x}O_{2+x}$ ($x \simeq 0$), were confirmed so far. If we assume 8/5 = 1.6 and 5/3 = 1.666 ... as the minimum and the maximum value for the tolerance range of a_1/a_2, possible phases are systematically given by the so-called Farey tree rule (Fig. 6), as was demonstrated by Perez-Mato *et al.* (1999). A phase with the ratio $a_1/a_2 = a_2^*/a_1^* = n/m$ is represented by [n/m]. Expected structures between [5/3] and [8/5] are [13/8], [18/11], [21/13], [23/14] ... from the figure.

As the chemical composition is AM_2X for the first substructure and M_2X_4 for the second substructure, the chemical composition for a whole crystal is generally given by $(AM_2X)_m(M_2X_4)_n = A_mM_{2(m+n)}X_{m+4n}$, where A is Sr^{2+} or Eu^{2+} and $m = a_1^*/a^* = a/a_1$ and $n = a_2^*/a^* = a/a_2$. Si/Al and O/N ratios are given by $A_m^{2+}Si_{-5m+6n-s}Al_{7m-4n+s}O_sN_{m+4n-s}$, so that the charge neutrality in a whole crystal is kept. The parameter s in this formula is equal to x in $Eu_3Si_{15-x}Al_{1+x}O_xN_{23-x}$ ($x \simeq 5/3$) of m = 3 and n = 5, while $Sr_5Al_{5+x}Si_{21-x}N_{35-x}O_{2+x}$ ($x \simeq 0$) of m = 5 and n = 8 is rewritten by $Sr_5Si_{23-s}Al_{3+s}O_sN_{37-s}$ ($s \simeq 2$). A predicted phase [13/8] is defined by m = 8 and n = 13, and the expected chemical composition is $A_8^{2+}Si_{38-s}Al_{4+s}O_sN_{60-s}$.

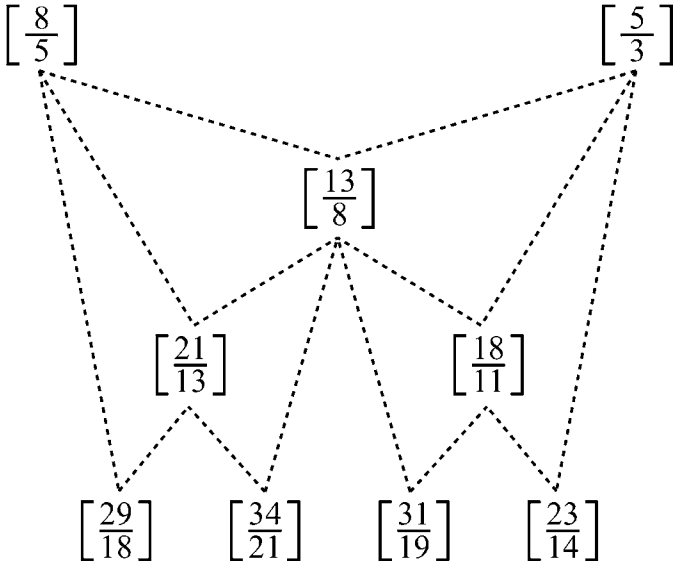

Figure 6
Scheme of the Farey tree between 8/5 and 5/3. A phase [n/m] is defined from the two generators indicated by dotted lines, [n_1/m_1] and [n_2/m_2], as [n/m] = [$(n_1 + n_2)/(m_1 + m_2)$].

The splitting of M sites is systematically treated in the (3 + 1)-dimensional description, which is one of the advantages of using the (3 + 1)-dimensional model. If the splitting of M1_1 is ignored, the occupation domains for M1_1a–M1_1d in Table 5 can be united to a normal (that is, the occupation function is not the crenel function) site extending along the fourth direction. The M1_1 site in a basic structure is expressed by a straight line going through a point (x_1, x_2, x_3) = (1/4, 0.17665, 0.52295). (Fractional coordinates x_2 and x_3 are taken as the average value of those for M1_1a and M1_1b.) From this (3 + 1)-dimensional model, interatomic distances between M1_1 and X are given in Fig. 7(a), in which displacive modulations are ignored. The M1_1 site is in a distorted trigonal–bipyramidal coordination at around x_4 = 1/4 and x_4 =

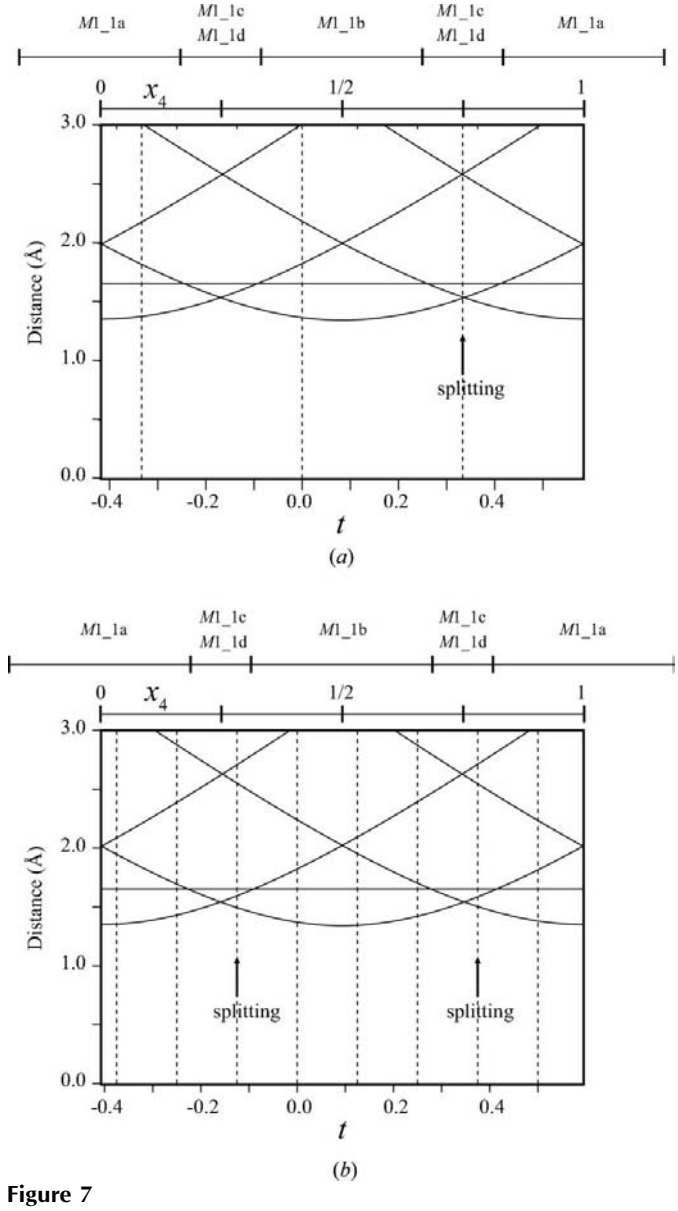

Figure 7
M1_1–X distances from a (3 + 1)-dimensional structure model for (a) α = 5/3 and (b) α = 13/8, assuming no splitting for the M sites. $t = x_4 - \alpha x_1$. M sites on the three-dimensional section t_0 = 0 are indicated by dotted lines. Displacive modulations are ignored.

3/4, as seen in the figure. (Note that $t = x_4 - \alpha x_1 = x_4 - 5/12$ for $\alpha = 5/3$ and $x_1 = 1/4$.) Two apical bonds are too long to stabilize the M (Si or Al) ion. Therefore, the M ion needs to shift toward either of the two apical X ions, which means the splitting of the site. Therefore, occupation domains corresponding to the regions around $x_4 = 1/4$ and $x_4 = 3/4$ are allotted for $M1$_1c and $M1$_1d in the split model, as indicated in the upper part of the figure. One of the $M1$_1 sites on the three-dimensional section indicated by an arrow in the figure splits in a real structure. The basic trends of the plots in Fig. 7(*a*) as functions of x_4 are unaffected by the wavevector component α ($= a_1/a_2$). Therefore, occupation domains around $x_4 = 1/4$ and $x_4 = 3/4$ are always allotted for split M sites in the (3 + 1)-dimensional model.

$M1$_1—X distances for $\alpha = 13/8$ are in Fig. 7(*b*), which is drawn in the same manner as for $\alpha = 5/3$ in Fig. 7(*a*). Among eight M sites on the three-dimensional section $t_0 = 0$, two sites are considered as in a distorted trigonal-bipyramidal coordination with two long apical bonds, which are expected to split, as indicated in the figure. Consequently, the width of the occupation domain Δ is set to 3/8 for $M1$_1a and $M1$_1b, and 1/8 for $M1$_1c and $M1$_1d, as shown in the upper part of Fig. 7(*b*). A similar consideration is to be made for $M1$_2a–$M1$_2d. Thus, a basic model considering the M site splitting for the [13/8] phase at the three-dimensional section $t_0 = 0$ is given in Fig. 8. A space group for the [13/8] phase, that is a = odd/even, is $P2_1$ at this three-dimensional section. Space groups Pm (with the unique axis **a**) and $P1$ are also possible, as listed in Table 4. The cell dimensions are estimated to be $a \simeq 2.94 \times n = 2.94 \times 13 \simeq 38.2$, $b \simeq 9.0$, $c \simeq 7.5$ Å, and a slight deviation from 90° may be found in angle(s) according to space group. Twinning is likely to occur in all cases.

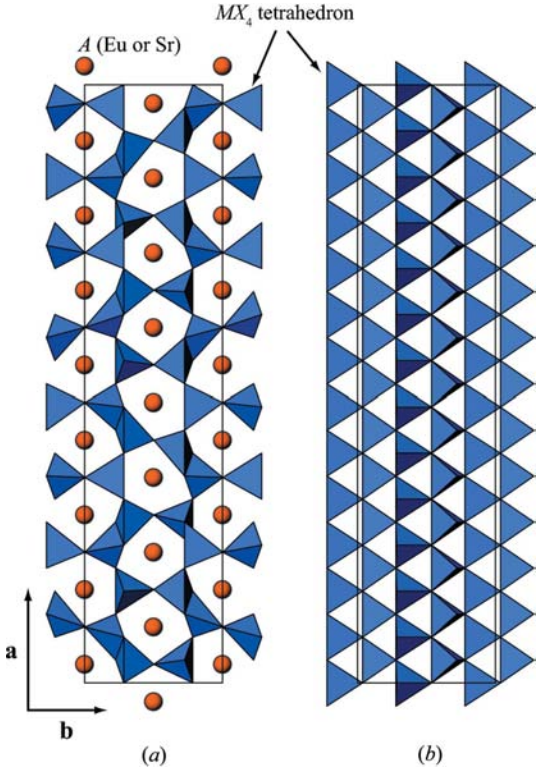

Figure 8
Projection along **c** of (*a*) the first framework unit and guest ions, and (*b*) the second framework unit in a basic model for a predicted phase of commensurate composite crystal $A_8^{2+}Si_{38-s}Al_{4+s}O_sN_{60-s}$ with $\alpha = 13/8$. Structure parameters used are in Table 5, except that Δ is 3/8 for $M1$_1a, $M1$_1b, $M1$_2a and $M1$_2b, and 1/8 for $M1$_1c, $M1$_1d, $M1$_2c and $M1$_2d. $M1$_1c and $M1$_2c are occupied, but $M1$_1d and $M1$_2d are vacant as an example of the possible local structure.

One of the unusual features in structures of this series is the formation of edge-sharing tetrahedra. Among 12 MX_4 tetrahedra within a unit cell for the phase of $\alpha = 5/3$ in Fig. 2(*a*), eight tetrahedra are connected by sharing the edge. For the predicted phase of $\alpha = 13/8$ in Fig. 8(*a*), 24 of 32 tetrahedra are edge-sharing. For $Sr_5Al_{5+x}Si_{21-x}N_{35-x}O_{2+x}$ with an $\alpha = 8/5$ phase (Oeckler *et al.*, 2009), 16 out of 20 tetrahedra in the corresponding framework unit are edge-sharing. Thus, the ratio of the number of edge-sharing tetrahedra to that of all tetrahedra in the first framework unit is 2/3, 3/4 and 4/5 for $\alpha =$ 5/3, 13/8 and 8/5. That is, the ratio of edge-sharing tetrahedra increases with decreasing α. This relation is explained as follows. The ratio of edge-sharing tetrahedra generally depends on the M/X ratio (*i.e.* the ratio of the number of M ions to that of X ions) constructing the framework unit. That is, the higher the M/X ratio, the higher the ratio of edge-sharing tetrahedra. The M ions constructing the first framework unit (Figs. 2*a* and 8*a*), $M1$_1a, $M1$_1b, $M1$_2a and $M1$_2b, belong to the first substructure in the composite crystal model, while most of the anions in this framework unit, N2_1 and N2_2, belong to the second substructure. As α is the ratio of the basic periods for the two substructures a_1/a_2, the smaller α (*i.e.* the lower a_1/a_2 ratio) leads to the higher M/X ratio in the framework unit and consequently the higher ratio of edge-sharing tetrahedra.

We can also consider phases which are not given in Fig. 6, such as [3/2], [7/4], [11/6] and [11/7], although the possibility for obtaining these structures is unclear because all of these fractions (*i.e.* the a_1/a_2 ratio in each structure) are out of the range between 8/5 and 5/3. In the same manner as shown above, chemical composition, possible space groups, cell parameters and the initial structure model are given for any phases in the series. Using the (3 + 1)-dimensional model, the number of parameters may be reduced in refinements of long-period structures. Incommensurate phases might be possible, as suggested by Oeckler *et al.* (2009) from electron diffraction experiments, although it is difficult to experimentally discriminate an incommensurate phase from long-period structures. The (3 + 1)-dimensional model based on Table 5 can also be used as a basic model for the refinement of incommensurate phases.

Recently an Eu-doped Sr-SiAlON phosphor, $Sr_3Si_{13}Al_3O_2N_{21}$, with an orthorhombic unit cell of $a = 9.037$, $b = 14.734$, $c = 7.464$ Å, was reported (Fukuda *et al.*, 2008, 2009). It was mentioned that four kinds of framework unit belonging to a space group $P2_1$ were seen, but the whole structure had the orthorhombic symmetry of the space group $P2_12_12_1$. From the projections given in their papers, it seems that the framework structure is similar to that of

$Eu_3Si_{15-x}Al_{1+x}O_xN_{23-x}$ ($x \simeq 5/3$). However, no structure parameters for this Sr-SiAlON are given. The validity of the space group $P2_12_12_1$ is still unclear, as no experimental details, such as final reliability factors, are given. Thus, meaningful discussion about structural relations between $Sr_3Si_{13}Al_3O_2N_{21}$ and $Eu_3Si_{15-x}Al_{1+x}O_xN_{23-x}$ ($x \simeq 5/3$) is impossible at this stage.

In summary, a new Eu-SiAlON, $Eu_3Si_{15-x}Al_{1+x}O_xN_{23-x}$ ($x \simeq 5/3$), was synthesized and the structure was determined using a twinned sample. As two substructures with different periodicities are seen in the structure, this Eu-SiAlON is considered to be a commensurate composite crystal. The structure of the present Eu-SiAlON with space group $P2_1$ is closely related to that of an Eu-doped Sr_5Al_{5+x}-$Si_{21-x}N_{35-x}O_{2+x}$ ($x \simeq 0$; Oeckler *et al.*, 2009) with space group $Pm2_1n$. A structure model in (3 + 1)-dimensional space was proposed, from which the two structures are derived despite different crystal systems and space groups. Possible commensurate phases belonging to the series were presented. It was demonstrated that the chemical composition, space group, cell parameters and the basic structure model for those phases can be given by the composite crystal model, which is helpful in studing this series of SiAlON further.

The authors are grateful to Mr Kosuke Kosuda at NIMS for performing EPMA.

References

Bagautdinov, B., Pilz, K., Ludecke, J. & van Smaalen, S. (1999). *Acta Cryst.* B**55**, 886–895.

Brown, I. D. (1996). *J. Appl. Cryst.* **29**, 479–480.

Dowty, E. (2005). *ATOMS*. Shape Software, Kingsport, Tennessee, USA.

Esmaeilzadeh, S., Grins, J., Shen, Z., Eden, M. & Thiaux, M. (2004). *Chem. Mater.* **16**, 2113–2120.

Fukuda, Y., Ishida, K., Mitsuishi, I. & Nunoue, S. (2009). *Appl. Phys. Express*, **2**, 012401.

Fukuda, Y., Mitsuishi, I. & Nunoue, S. (2008). *Proc. 15th Int. Display Workshops*, pp. 803–806.

Hirosaki, N., Xie, R.-J., Kimoto, K., Sekiguchi, T., Yamamoto, Y., Suehiro, T. & Mitomo, M. (2005). *Appl. Phys. Lett.* **86**, 211905.

Janner, A. & Janssen, T. (1980*a*). *Acta Cryst.* A**36**, 399–408.

Janner, A. & Janssen, T. (1980*b*). *Acta Cryst.* A**36**, 408–415.

Janssen, T., Janner, A., Looijenga-Vos, A. & de Wolff, P. M. (1999). *International Tables for Crystallography*, edited by A. J. Wilson, Vol. C, pp. 899–947. Dordrecht: Kluwer Academic Publishers.

Krevel, J. W. H. van, van Rutten, J. W. T., Mandal, H., Hintzen, H. T. & Metselaar, R. (2002). *J. Solid State Chem.* **165**, 19–24.

Lauterbach, R., Irran, E., Henry, P. H., Weller, M. T. & Schnick, W. (2000). *J. Mater. Chem.* **10**, 1357–1364.

Lauterbach, R. & Schnick, W. (1998). *Z. Anorg. Allg. Chem.* **624**, 1154–1158.

Lauterbach, R. & Schnick, W. (2000). *Solid State Sci.* **2**, 463–472.

Momma, K. & Izumi, F. (2008). *J. Appl. Cryst.* **41**, 653–658.

Oeckler, O., Kechele, J. A., Koss, H., Schmidt, P. J. & Schnick, W. (2009). *Chem. Eur. J.* **15**, 5311–5319.

Palatinus, L. & Chapuis, G. (2007). *J. Appl. Cryst.* **40**, 786–790.

Perez-Mato, J. M., Madariaga, G., Zuñiga, F. J. & Garcia Arribas, A. (1987). *Acta Cryst.* A**43**, 216–226.

Perez-Mato, J. M., Zakhour-Nakhl, M., Weill, F. & Darriet, J. (1999). *J. Mater. Chem.* **9**, 2795–2808.

Petricek, V., Dusek, M. & Palatinus, L. (2006). *JANA*2006. Institute of Physics, Praha, Czech Republic.

Sheldrick, G. M. (1996). *SADABS*. University of Gottingen, Germany.

Shen, Z., Grins, J., Esmaeilzadeh, S. & Ehrenberg, H. (1999). *J. Mater. Chem.* **9**, 1019–1022.

Smaalen, S. van (1987). *Acta Cryst.* A**43**, 202–207.

Smaalen, S. van (1995). *Cryst. Rev.* **4**, 79–202.

Tanaka, M., Katsuya, Y. & Yamamoto, A. (2008). *Rev. Sci. Instrum.* **79**, 075106–075111.

Wolff, P. M. de (1974). *Acta Cryst.* A**30**, 777–785.

Xie, R.-J., Hirosaki, N., Mitomo, M., Yamamoto, Y., Suehiro, T. & Sakuma, K. (2004). *J. Phys. Chem. B*, **108**, 12027–12031.

Xie, R.-J., Hirosaki, N., Sakuma, K., Yamamoto, Y. & Mitomo, M. (2004). *Appl. Phys. Lett.* **84**, 5404–5406.

Xie, R.-J., Mitomo, M., Uheda, K., Xu, F.-F. & Akimune, Y. (2002). *J. Am. Ceram. Soc.* **85**, 1229–1234.

Yamamoto, A. (1996). *Acta Cryst.* A**52**, 509–560.

Yamamoto, A., Janssen, T., Janner, A. & de Wolff, P. M. (1985). *Acta Cryst.* A**41**, 528–530.